

Micelle Tailor

Size & Agg. Number
Chain Exchange
CMC



⊕ Random Micelle ⊕

⊕ Alternating Micelle ⊕

Back-order

ISSN 1759-9962



Cite this: *Polym. Chem.*, 2025, **16**, 652

Precisely controlled yet dynamically exchanged micelles *via* the self-assembly of amphiphilic acrylate random copolymers in water†

Hiroyuki Kono,  Makoto Ouchi  and Takaya Terashima *

Herein, we investigated the self-assembly of amphiphilic acrylate random copolymers bearing hydrophilic poly(ethylene glycol) chains and hydrophobic dodecyl groups into micelles in water. The random copolymers formed precise yet dynamic micelles in water, dependent on the degree of polymerization (DP) and composition. The copolymers shorter than a threshold DP_{th} exclusively formed multichain micelles and the copolymers longer than the DP_{th} self-folded into unimer micelles. The molecular weight and size of the multichain micelles were determined by the composition, and the aggregation number was controllable by the DP. The critical micelle concentration of the random copolymers was estimated to be approximately $1 \times 10^{-3} \text{ mg mL}^{-1}$, and almost independent of the DP, aggregation number, monomer sequence, and backbone structures. More uniquely, owing to the flexible backbones, the acrylate random copolymer micelles induced the exchange of polymer chains even at a low temperature such as $10 \text{ }^\circ\text{C}$ (activation energy: $E_a = \sim 40 \text{ kJ mol}^{-1}$) although their corresponding methacrylate counterparts with relatively rigid backbones required at least $25 \text{ }^\circ\text{C}$ for polymer chain exchange.

Received 11th November 2024,
Accepted 19th December 2024

DOI: 10.1039/d4py01272k

rsc.li/polymers

Introduction

Self-assembly of amphiphilic polymers and molecules in water is a key strategy to produce nanostructured objects such as micelles, vesicles, and single-chain polymer nanoparticles.^{1–16} These self-assemblies are useful as functional materials including stimuli-responsive materials,^{17–19} molecular encapsulation/release materials,^{20,21} and drug-delivery vehicles.^{22,23} In general, polymer or surfactant micelles and related aggregates are formed in water *via* hydrophobic effects or physical interactions above the critical micelle or aggregation concentration. These self-assemblies often induce the exchange of the polymer chains or molecules among each other; the dynamic behaviour depends on the molecular structures, solution temperature, solute concentration, and additives in solutions. Controlling not only the size and three-dimensional architectures but also dynamic properties is crucial in designing self-assembled materials with desired properties and functions.

To date, various amphiphilic polymers with distinct structures, such as block,^{1–3,5–8,24–27} random/statistical,^{28–43} and

alternating^{44–48} copolymers, have been designed for targeted self-assemblies. Among them, random copolymers have attracted attention as scaffolds for small micelles or SCNPs whose size is about 10 nm and close to that of proteins. We have developed self-assembly systems of amphiphilic random copolymers bearing hydrophilic poly(ethylene glycol) (PEG) and hydrophobic alkyl groups [*e.g.*, PEG methyl ether methacrylate (PEGMA)/dodecyl methacrylate (DMA) random copolymers (Fig. 1)].^{35–43} These copolymers form micelles *via* chain-folding by the association of hydrophobic side chains in water and show unique self-assembly behaviour in water, depending on the degree of polymerization (DP): the copolymers shorter than a threshold DP_{th} exclusively form multichain micelles *via* intermolecular self-assembly and those longer than the DP_{th} form unimer micelles *via* self-folding.^{35,39,40} The size of the multichain micelles is determined by the copolymer composition and side chain structures, irrespective of the DP. Additionally, the random copolymer micelles show dynamic chain-exchange behaviour, depending on the side chains and temperature.^{41–43}

Self-assembly of amphiphilic copolymers is also dependent on the main chain structures and monomer sequence. For instance, the alternating copolymer of PEG methyl ether acrylate (PEGA) and dodecyl vinyl ether (DVE)⁴⁸ forms a multichain micelle with molecular weight lower than the corresponding methacrylate³⁵ or acrylate³⁶ random copolymers with the same composition of PEG and dodecyl side chains. This is probably

Department of Polymer Chemistry, Graduate School of Engineering, Kyoto University, Katsura, Nishikyo-ku, Kyoto 615-8510, Japan.

E-mail: terashima.takaya.2e@kyoto-u.ac.jp

† Electronic supplementary information (ESI) available: Experimental details of the synthesis and characterization of polymers, and SEC, NMR, DLS, and fluorescence spectroscopy. See DOI: <https://doi.org/10.1039/d4py01272k>

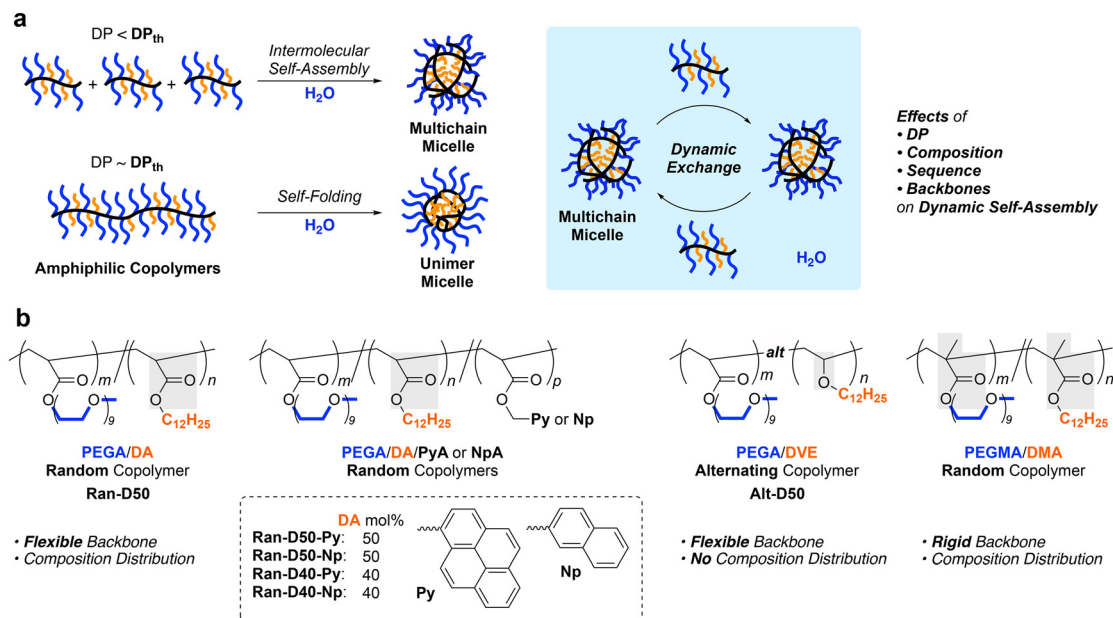


Fig. 1 (a) Precision self-assembly of amphiphilic copolymers into multichain or unimer micelles in water, depending on the degree of polymerization (DP), and dynamic exchange of polymer chains between micelles. (b) Design of acrylate random, acrylate/vinyl ether alternating, and methacrylate random copolymers with hydrophilic poly(ethylene)glycol (PEG) chains and hydrophobic dodecyl groups.

because the alternating copolymer has a flexible acrylate/vinyl ether backbone and does not contain consecutive dodecyl units. Acrylamide random copolymers consisting of more hydrophilic backbones also formed micelles with molecular weights lower than those of their acrylate counterparts.³⁸ These results suggest that the flexibility and polarity of the polymer backbones affect the dynamic properties of polymer micelles. Owing to the flexible backbones, amphiphilic acrylate random copolymers^{36,37} are expected to induce precise yet dynamic self-assembly into size-controlled micelles that may promote chain exchange more than methacrylate copolymer micelles.^{41–43}

Herein, we investigated the self-assembly of amphiphilic acrylate random copolymers bearing PEG chains and dodecyl groups into micelles in water, focusing on the effects of the DP, composition, and sequence distribution on the size and aggregation number of the micelles, critical micelle concentration (CMC), and chain exchange properties (Fig. 1). The random copolymers were obtained from free radical copolymerization of hydrophilic PEGA and hydrophobic dodecyl acrylate (DA) in the presence or absence of small amounts of pyrene (Py) or naphthalene (Np)-bearing acrylates (PyA or NpA). The copolymers with broad dispersity (D) were fractionated into samples with different molecular weights and narrow D by preparative size-exclusion chromatography (SEC). The aqueous solutions of the fractionated copolymers were analyzed by SEC with multiangle laser light scattering (MALLS) to determine the absolute weight-average molecular weight and aggregation number of the micelles. The chain exchange between their micelles was evaluated by fluorescence measurements of the mixtures of Py or Np-labeled copolymers.

The acrylate random copolymers, as well as methacrylate counterparts,^{35,39,40} induced self-assembly controlled by the DP and composition. The copolymers with a DP smaller than a threshold DP_{th} formed multichain micelles whose size was constant and independent of DP. In contrast, the copolymers with a DP larger than DP_{th} mainly formed unimer micelles. The size of multichain micelles increased with increasing content of dodecyl groups. The CMC of the random copolymers in water was estimated to be approximately 1.0×10^{-3} mg mL⁻¹, independent of the DP (*i.e.*, aggregation number) and monomer sequence distribution (random or alternating). Uniquely, the acrylate random copolymers induced chain exchange even at a low temperature more efficiently than their methacrylate counterparts.

Results and discussion

Synthesis of amphiphilic random copolymers

Amphiphilic random copolyacrylates bearing hydrophilic PEG chains, hydrophobic dodecyl groups, and a small amount (~1 mol%) of pyrene (Py) or naphthalene (Np) units were synthesized by free radical copolymerization of PEGA, DA, PyA or NpA with 2,2'-azobis(isobutyronitrile) in toluene at 60 °C. The DA content was set to 40 or 50 mol% to examine the effects of composition, main chain structures, and monomer sequence (random *vs.* alternating) on self-assembly behaviour. The Py or Np fluorophores were used to evaluate the exchange of the polymer chains between their micelles in water by fluorescence resonance energy transfer (FRET). The random copolymers are coded as **Ran-D40-Py** or **Np** and **Ran-D50-Py** or **Np**, dependent

on the DA content and the Py or Np labels. A non-labeled PEGA/DA random copolymer with 50 mol% DA (**Ran-D50**) was also prepared to investigate the CMC in water.

In all the copolymerization, both PEGA and DA were simultaneously consumed at the same rate, regardless of the feed ratio of their monomers. This indicates that the two monomers are randomly distributed in the resulting copolymer chains (Fig. S1†). The random copolymers were analyzed by SEC in *N,N*-dimethylformamide (DMF) containing 10 mM LiBr. The copolymers had number-average molecular weight (M_n) values of 23 400–34 000 g mol⁻¹ and dispersity values ($D = M_w/M_n$; molecular weight distribution) of 2.05–2.43 by poly(methyl methacrylate) (PMMA) standard calibration (Fig. S1†) or M_n values of 10 500–15 600 g mol⁻¹ and D values of 2.36–2.86 by poly(ethylene oxide) (PEO) standard calibration (Fig. 2a, S2 and S3†). To examine the effects of the monomer sequence distribution and backbone structures on the CMC, a PEGA/DVE alternating copolymer (**Alt-D50**, $M_n = 33\,500$ g mol⁻¹, $D = 1.72$ by PMMA calibration or $M_n = 15\,600$ g mol⁻¹, $D = 1.89$ by PEO calibration) was also prepared by free radical copolymerization of PEGA in the presence of an excess of DVE according to the literature.⁴⁶ The alternating sequence of PEGA and DVE was confirmed by ¹³C NMR spectroscopy (Fig. S4†).

All the copolymers with broad dispersity were fractionated using a preparative SEC into six samples (A–F) with different molecular weights (Fig. 2 and S2, S3†). The chemical structures and compositions of the fractionated copolymers were analyzed by ¹H NMR spectroscopy (Fig. S5–S10 and Tables S1–S4†). The absolute weight-average molecular weight ($M_{w,DMF}$) and D_{DMF} of the fractionated copolymers were determined using an SEC system equipped with a MALLS detector in DMF (10 mM LiBr) as an eluent, where the copolymers are unimolecularly dissolved in DMF. The degree of polymerization (DP) of the fractionated copolymers was calculated from the $M_{w,DMF}$ and D_{DMF} (by SEC-MALLS), the composition (by ¹H NMR), and the formula weight of monomers (Tables S1–S4†). Typically, **Ran-D50-F–A** ($M_n = 4500$ – $90\,700$ g mol⁻¹, $D = 1.16$ – 1.91 by SEC with PEO calibration, Fig. 2c) had a DP of 55–799.

Self-assembly of amphiphilic random copolymers into micelles in water

The self-assembly of amphiphilic random copolymers (**Ran-D50**, **Ran-D50-Py** or **Np**, **Ran-D40-Py** or **Np**) into micelles in water was evaluated using SEC-MALLS in H₂O containing 100 mM NaCl as an eluent. The aqueous solutions of the copolymers were prepared as follows: in vials, the copolymers were dissolved in water at 25 °C (1 mg mL⁻¹), giving transparent solutions. The solutions were sonicated at 25 °C for 3 min (sonicator: Branson, Bransonic 1510) and filtered through a poly(tetrafluoroethylene) membrane filter (0.45 μm, Merck Millipore) before analysis. The aqueous solutions were injected into the SEC system to determine M_n (apparent size), absolute weight-average molecular weight (M_{w,H_2O}), and D of the polymer micelles in water (Tables S1–S4†). The apparent size of the micelles was evaluated with M_n determined by SEC in



Fig. 2 SEC curves of **Ran-D50** in (a) DMF (10 mM LiBr) and (b) H₂O (100 mM NaCl) with PEO standard calibration. **Ran-D50** was fractionated into six samples with different molecular weights (A–F) by preparative SEC. (c and d) SEC curves of fractionated **Ran-D50-A–F** with different DPs in (c) DMF (10 mM LiBr) and (d) H₂O (100 mM NaCl). The M_n and D values are determined with PEO standard calibration.

water with PEO calibration. The M_{w,H_2O} of the micelles was determined by SEC-MALLS in water to estimate the aggregation number (N_{agg}) of the copolymers [$N_{agg} = M_{w,H_2O}$ (MALLS)/ $M_{w,DMF}$ (MALLS)]. The D of the micelles was determined by PEO calibration or MALLS.

Effects of the DP on apparent micelle size. The aqueous solution of **Ran-D50** with broad dispersity ($D = 2.60$ in DMF, Fig. 2a) was first analyzed by SEC in water containing 100 mM NaCl. **Ran-D50** showed a unimodal SEC curve with narrow dispersity in water ($D = 1.08$, Fig. 2b). This implies that the acrylate-based **Ran-D50**, as well as methacrylate-based PEG/dodecyl random copolymers³⁵ and PEGA/DVE alternating copolymers,⁴⁸ form micelles whose apparent size is primarily determined by the composition. Then, fractionated **Ran-D50-A–F** with different DPs were analyzed by SEC in water (Fig. 2d). **Ran-D50-F–C** with 55–270 DP showed unimodal SEC curves with almost identical M_n (20 100–22 700 g mol⁻¹) and narrow dispersity (1.06–1.08) by PEO calibration, whereas **Ran-D50-B** and **A** with DP values more than 457 showed a shift of their SEC curves to high molecular weight with increasing DP. This result suggests that **Ran-D50** with a DP smaller than 270 forms multi-chain micelles whose size is independent of the DP and **Ran-D50** with a DP larger than at least about 450 mostly forms unimer micelles whose size increased with the DP.

Fractionated **Ran-D50-Py** or **Np** with a DP smaller than approximately 270 also showed SEC curves with almost identical M_n (Fig. 3a and S11[†]). This supports the fact that a small

amount (~ 1 mol%) of Py or Np labels hardly affects the self-assembly behaviour of the copolymers and the apparent size of the resulting micelles. In contrast, the copolymer composition affected the self-assembly and apparent size of micelles. Typically, **Ran-D40-Py-F-C** with a DP smaller than 160 showed SEC curves with almost identical M_n (Fig. 3b and S12), whereas the M_n was smaller than that for constant size micelles of **Ran-D50(-Py or Np)**. In addition, the threshold DP of the constant size micelles for **Ran-D40-Py** was smaller than that for **Ran-D50-Py**.

Absolute molecular weight and aggregation number. The M_{w,H_2O} of the polymer micelles was determined by SEC-MALLS in water. The M_{w,H_2O} for **Ran-D50-F-C** with 55–270 DP was nearly constant around $200\,000\text{ g mol}^{-1}$ and their N_{agg} values decreased from 6.6 to 1.9 with increasing DP (Fig. 4a). In contrast, the M_{w,H_2O} for **Ran-D50-B** and **A** with a DP more than 457 increased with increasing DP and their N_{agg} values were close to 1. As confirmed by dynamic light scattering in water, the hydrodynamic radius (R_h) of **Ran-D50-F-C** micelles was also almost constant in the range of 5.7–6.1 nm, independent of the DP of the copolymers, whereas the R_h for **Ran-D50-B** and **A** micelles increased from 6.2 nm to 7.7 nm with increasing DP (Fig. S13 and Table S1[†]). These results demonstrate that, as implied by M_n (apparent size by PEO calibration), **Ran-D50** copolymers have a threshold DP (DP_{th}) of approximately 400 between multichain micelles and unimer micelles: (1) the copolymers with a DP smaller than that of DP_{th} exclusively induce the intermolecular association of the polymer chains to form multichain micelles ($N_{agg} > 2$) with constant M_{w,H_2O} and R_h , where the N_{agg} of the micelles decreases with increasing



Fig. 3 SEC curves of (a) **Ran-D50-Py-A-F** and (b) **Ran-D40-Py-A-F** with different molecular weights in DMF (black lines) and H_2O (blue lines).



Fig. 4 Absolute weight-average molecular weight (M_w , determined by SEC-MALLS) of (a) **Ran-D50-A-F**, (b) **Ran-D50-Py-A-F**, (c) **Ran-D50-Np-A-F**, (d) **Alt-D50-A-F**, (e) **Ran-D40-Py-A-F**, and (f) **Ran-D40-Np-A-F** in water (100 mM NaCl, blue) or DMF (10 mM LiBr, black) as a function of the DP. Aggregation number: $N_{agg} = M_{w,H_2O}/M_{w,DMF}$.

DP. (2) The copolymers with a DP larger than the DP_{th} mostly induce self-folding into unimer micelles whose M_{w,H_2O} and R_h increase with increasing DP. Py or Np-labeled **Ran-D50-F-C** with a DP smaller than DP_{th} also formed multichain micelles with M_{w,H_2O} ($\sim 200\,000\text{ g mol}^{-1}$) that is close to those of non-labelled **Ran-D50-F-C** (Fig. 4b and c).

In contrast, **Ran-D40-Py** (or **Np**)-**F-C** with a DP smaller than about 160 formed multichain micelles with a constant M_{w,H_2O} of approximately $100\,000\text{ g mol}^{-1}$ and **Ran-D40-Py** (or **Np**)-**B** and **A** with a DP larger than about 300 formed unimer micelles whose M_{w,H_2O} increased with increasing DP (Fig. 4e and f). The constant M_{w,H_2O} and DP_{th} of their **Ran-D40** multichain micelles were smaller than those of their **Ran-D50** counterparts, indicating that more hydrophilic polymers form smaller micelles. This trend is consistent with the self-assembly of methacrylate-based amphiphilic random copolymers into micelles.^{35,39} Furthermore, the constant M_{w,H_2O} of **Alt-D50** multichain micelles ($\sim 90\,000\text{ g mol}^{-1}$, Fig. 4d) was smaller than that of their **Ran-D50** counterparts ($\sim 200\,000\text{ g mol}^{-1}$). This is probably because the alternating copolymers have flexible vinyl ether backbones and have no consecutive sequence of dodecyl side chains to afford the efficient folding of polymer chains into more compact micelles.⁴⁸

Critical micelle concentration of amphiphilic random or alternating copolymers

We examined the effects of the monomer sequence and DP (related to N_{agg}) on the CMC of amphiphilic random or alternating copolymers. **Ran-D50** and **Alt-D50**, both of which have no fluorescent labels, were used. The CMC of the copolymers in water was determined by fluorescence spectroscopy with pyrene as follows:^{41,49,50} aqueous mixtures of the copolymers with different concentrations (1.0×10^{-4} – $1.0 \times 10^{-1}\text{ mg mL}^{-1}$) and a small amount of pyrene ($5 \times 10^{-7}\text{ M}$) were prepared, and the fluorescence spectra of the mixtures were measured at $25\text{ }^\circ\text{C}$ (Fig. 5 and S15[†]). The emission intensity ratio of I_1 (at 373 nm) and I_3 (at 384 nm) [I_1/I_3] was plotted as a function of the polymer concentration. CMC was defined as a concentration at which I_1/I_3 starts to decrease with increasing polymer concentration (Fig. 5).

As shown in Fig. 5a, the I_3 intensity (normalized by I_1) for the aqueous solutions of **Ran-D50-D** with DP 201 was almost constant up to approximately $1 \times 10^{-3}\text{ mg mL}^{-1}$ and increased with increasing polymer concentration above $1 \times 10^{-3}\text{ mg mL}^{-1}$. From the intersection concentration of the constant or decreasing I_1/I_3 values, the CMC was determined to be approximately $1 \times 10^{-3}\text{ mg mL}^{-1}$ (Fig. 5d). Similarly, the CMC of **Ran-**



Fig. 5 CMC of amphiphilic random or alternating copolymers in water. (a and f) Emission spectra of pyrene ($5 \times 10^{-7}\text{ M}$; normalized by I_1) containing (a) **Ran-D50-D** and (f) **Alt-D50-E** in water. (b–e and g–j) I_1/I_3 plots as a function of the polymer concentration (1.0×10^{-4} – $1.0 \times 10^{-1}\text{ mg mL}^{-1}$) of (b) **Ran-D50**, (c) **Ran-D50-A**, (d) **Ran-D50-D**, (e) **Ran-D50-F**, (g) **Alt-D50**, (h) **Alt-D50-A**, (i) **Alt-D50-E**, and (j) **Alt-D50-F**.

D50 with broad dispersity, **Ran-D50-A** with a DP of 799, and **Ran-D50-F** with a DP of 55 was approximately 1×10^{-3} mg mL⁻¹ (Fig. 5b, c and e). Though **Ran-D50-A**, **D**, and **F** form micelles with N_{agg} values of 1.2, 2.4, and 6.6 in water, respectively, the CMC was independent of their N_{agg} values. This is consistent with the fact that a **Ran-D50** micelle with broad N_{agg} distribution due to broad dispersity ($D = 2.60$) also has a close CMC. The CMC of amphiphilic alternating copolymers (**Alt-D50** with broad dispersity, **Alt-D50-A** with a DP of 497, **Alt-D50-E** with a DP of 109, and **Alt-D50-F** with a DP of 60) was also estimated to be 1×10^{-3} mg mL⁻¹, independent of N_{agg} (Fig. 5f–j). These CMC values were close to those of poly(styrene-ethylene oxide) block copolymer micelles.⁵⁰

In general, amphiphilic copolymers bearing hydrophilic and hydrophobic segments in water are placed at the air/water interface and dispersed as unimer chains or self-assemblies of multiple polymer chains in water.^{51,52} The three modes are dynamically exchanged in the equilibrium state, depending on the polymer concentration (Fig. 6a). At very low concentration, amphiphilic polymer chains are primarily located at the air/water interface, where the hydrophobic alkyl groups with low surface free energy are directed to the air. As the concentration increases, the amount of polymer chains at the interface increases. Once the interface is saturated, the polymer chains are not only dispersed as unimer chains in water but also form self-assemblies such as micelles *via* the association of hydrophobic groups above a concentration called CMC.

The CMC of both the acrylate-random and acrylate/vinyl ether alternating copolymers ($\sim 1.0 \times 10^{-3}$ mg mL⁻¹) was close to that of a methacrylate-random copolymer bearing PEG chains and dodecyl groups.⁴¹ This result importantly demonstrates that the CMC of their amphiphilic copolymers is mainly determined by the structure and composition of the side chains, and is independent of the backbone structures

and monomer sequence. This is because the mass of copolymer chains potentially filling at the air/water interface and averaged hydrophobic/hydrophilic balance of the copolymer chains are independent of the DP and monomer sequence as far as the composition (the molar ratio of PEG and dodecyl groups) of the copolymers is identical. Another interesting finding is that unimer micelles of **Ran-D50-A** or **Alt-D50-A** also have a CMC of $\sim 1.0 \times 10^{-3}$ mg mL⁻¹ as determined by the fluorescence measurements using pyrene. This implies that the amphiphilic copolymers are primarily placed at the air/water interface below the CMC ($< \sim 1.0 \times 10^{-3}$ mg mL⁻¹) and immediately form unimer micelles in water above the concentration.

The aqueous solutions of **Ran-D50** and **Alt-D50** further showed fluorescence intensity stemming from the excimer emission of pyrene at around 470 nm (I_{470}) above their CMC ($\sim 1.0 \times 10^{-3}$ mg mL⁻¹). However, the emission intensity changed, in response to the polymer concentration (Fig. 5a and f). For example, the I_{470} of **Ran-D50-D** increased with increasing concentration up to 1.0×10^{-2} mg mL⁻¹ and again decreased with increasing concentration. This suggests that the number of pyrene molecules enclosed within each micelle changes as the number of micelles increases (Fig. 6b). When the polymer concentration is below the CMC, pyrene is molecularly dispersed in the water phase. This is also confirmed by the fact that the I_1/I_3 ratio of the aqueous solutions of pyrene containing the copolymers (below the CMC) is identical to that of the aqueous solution of pyrene alone (5×10^{-7} M, Fig. S15†). At a concentration slightly above the CMC, a few micelles formed in water enclose multiple pyrene molecules within the hydrophobic cores, leading to excimer emission. At a concentration much higher than the CMC, the pyrene molecules were fully dispersed within the multiple micelle cores, decreasing the excimer emission. These results indicate that amphiphilic random or alternating copolymer micelles can encapsulate hydrophobic molecules within their cores and are potentially applicable as nanocapsules.



Fig. 6 (a) Equilibrium of amphiphilic random or alternating copolymers in water among three states: polymer chains placed at the air/water interface and unimer chains/micelles or multichain micelles dispersed in water. (b) Effects of concentration on the encapsulation of pyrene molecules into micelles in water during CMC measurements.

Dynamic exchange of polymer chains between micelles

The dynamic properties of **Ran-D50** or **Ran-D40** micelles in water were investigated, focused on the effects of copolymer composition (dodecyl groups: 50 or 40 mol%), DP (related to N_{agg}), and temperature on the exchange of the acrylate-copolymer chains. The chain exchange was analyzed by FRET in the mixtures of a Py-labeled micelle and a Np-labeled micelle.^{41,42} The aqueous solution of a Py-labeled micelle was mixed with that of a Np-labeled micelle ([polymer] = 1.0 mg mL⁻¹, Fig. 7a). Then, fluorescence measurement of the resulting mixture was immediately performed at various temperatures (10–35 °C), where the excitation wavelength for the Np units was set at 290 nm. The fluorescence intensity was monitored at 336 nm for the Np units (I_{Np}) and at 396 nm for the Py units (I_{Py}). The Förster radius of Np and Py is 2.86 nm.³⁰ Since the labeled Np or Py units are located within the hydrophobic cores of small micelles ($R_{\text{h}} = \sim 6$ nm), the coexistence of Py-labeled copolymers and Np-labeled copolymers within single micelles can be evaluated by FRET.



Fig. 7 (a) Evaluation of polymer chain exchange between Py-labeled micelles and Np-labeled micelles by FRET. (b) Fluorescence spectra obtained from the aqueous mixture of a **Ran-D50-Py-D** micelle and a **Ran-D50-Np-D** micelle by excitation at 290 nm at 35 °C: [polymer] = 1.0 mg mL⁻¹. The fluorescence intensity was monitored at 396 nm (I_{Py}) and 336 nm (I_{Np}). (c) Arrhenius plots of k_{obs} for the chain exchange of the mixtures of (blue) **Ran-D50-Py-D** ($N_{agg} = 2$) and **Ran-D50-Np-D** ($N_{agg} = 2$), (green) **Ran-D40-Py-D** ($N_{agg} = 2$) and **Ran-D40-Np-D** ($N_{agg} = 2$), and (red) **Ran-D50-Py-F** ($N_{agg} = 5$) and **Ran-D50-Np-F** ($N_{agg} = 8$). (d) and (e) Effect of temperature on the chain exchange: normalized I_{Py} ($I_{Py, norm}$) and fitting curves for the chain exchange of the binary mixtures of (d) a **Ran-D50-Py-D** micelle ($N_{agg} = 2$) and a **Ran-D50-Np-D** micelle ($N_{agg} = 2$) or (e) a **Ran-D50-Py-F** micelle ($N_{agg} = 5$) and a **Ran-D50-Np-F** micelle ($N_{agg} = 8$) in water at 10–35 °C. (f) Effect of N_{agg} and composition on the chain exchange at 35 °C: the mixtures of (blue) **Ran-D50-Py-D** ($N_{agg} = 2$) and **Ran-D50-Np-D** ($N_{agg} = 2$), (green) **Ran-D40-Py-D** ($N_{agg} = 2$) and **Ran-D40-Np-D** ($N_{agg} = 2$), and (red) **Ran-D50-Py-F** ($N_{agg} = 5$) and **Ran-D50-Np-F** ($N_{agg} = 8$).

For example, in the mixture of a **Ran-D50-Py-D** (DP = 172, $N_{agg} = 2$) micelle and a **Ran-D50-Np-D** (DP = 170, $N_{agg} = 2$) micelle at 35 °C, I_{Py} increased and I_{Np} slightly decreased with increasing measurement time (Fig. 7b). This indicates that FRET from the Np units to the Py units occurs with time progress: namely, the Np-labeled polymer chains are gradually mixed with their Py-labeled counterparts to form Np- and Py-mixed micelles in water. Additionally, the mixture of **Ran-D40-Py-D** (DP = 91, $N_{agg} = 2$) micelle and **Ran-D40-Np-D** (DP = 82, $N_{agg} = 2$) or that of **Ran-D50-Py-F** (DP = 68, $N_{agg} = 5$) and **Ran-D50-Np-F** (DP = 38, $N_{agg} = 8$) also showed similar increase of I_{Py} and decrease of I_{Np} with time progress (Fig. S16–S18†). The chain exchange kinetics were thus evaluated from the I_{Py} values of the mixtures normalized over time $\{I_{Py}(t)\}$ using eqn (1):²⁴

$$I_{Py, norm} = \frac{I_{Py}(t) - I_{Py, \infty}}{I_{Py}(0) - I_{Py, \infty}} = 1 - \exp(-k_{obs}t) \quad (1)$$

where $I_{Py}(0)$ is the emission intensity from the Py units just after mixing ($t = 0$), and $I_{Py, \infty}$ is the intensity in the fully mixed state achieved after heating the mixture at 50 °C for 24 h, followed by setting to the measurement temperature. $I_{Py, norm}$ was plotted against time at various temperatures.

In all the cases, $I_{Py, norm}$ increased with time, and the increase of $I_{Py, norm}$ turned fast on increasing temperature (Fig. 7). This indicates that the exchange of the polymer chains is promoted upon heating the solutions. The initial $I_{Py, norm}$ values were fitted by eqn (1) to determine the apparent rate constant (k_{obs}) for the exchange of polymer chains between their micelles. The k_{obs} for the mixture of a **Ran-D50-Py-D** (DP = 172, $N_{agg} = 2$) micelle and a **Ran-D50-Np-D** (DP = 170, $N_{agg} = 2$) micelle at 35 °C ($3.0 \times 10^{-2} \text{ min}^{-1}$) was almost the same as that for a **Ran-D40-Py-D** (DP = 91, $N_{agg} = 2$) micelle and a **Ran-D40-Np-D** (DP = 82, $N_{agg} = 2$) micelle ($3.0 \times 10^{-2} \text{ min}^{-1}$), indicating that the 10 mol% difference in copolymer composition had little effect on the apparent exchange rate of polymer chains. In contrast, the k_{obs} for the mixture of a **Ran-D50-Py-F** (DP = 68, $N_{agg} = 5$) micelle and a **Ran-D50-Np-F** (DP = 38, $N_{agg} = 8$) micelle at 35 °C ($4.6 \times 10^{-2} \text{ min}^{-1}$) was larger than that for the mixtures of micelles with $N_{agg} = 2$. This means that the exchange rate of polymer chains increased with increasing N_{agg} ;⁴² namely, small DP polymers are more easily exchanged between micelles. In general, exchange of polymer chains between micelles occurs *via* unimer release/insertion, fragmentation of micelles, and micelle/micelle collision processes.^{24,27,43} Since the CMC of the random copolymers was independent of the DP, faster chain exchange of micelles

with a large N_{agg} may be promoted by fragmentation and/or collision processes of their micelles.

The k_{obs} values were applied to Arrhenius plots (Fig. 7c). The activation energy (E_a) for the chain exchange processes of **Ran-D50-Py-D** ($N_{\text{agg}} = 2$)/**Ran-D50-Np-D** ($N_{\text{agg}} = 2$) micelles, **Ran-D40-Py-D** ($N_{\text{agg}} = 2$)/**Ran-D40-Np-D** ($N_{\text{agg}} = 2$) micelles, and **Ran-D50-Py-F** ($N_{\text{agg}} = 5$)/**Ran-D50-Np-F** ($N_{\text{agg}} = 8$) micelles was estimated to be 35, 47, and 43 kJ mol⁻¹, respectively. The E_a values were almost independent of the composition and DP of their copolymers but significantly lower than the E_a for the chain exchange of methacrylate-based PEGMA/DMA (50/50 mol%) random copolymer micelles carrying identical PEG chains and dodecyl groups (141 kJ mol⁻¹, Fig. 1b).⁵³ This notably demonstrates that the flexible polyacrylate backbones easily induce the exchange of polymer chains between micelles with less temperature effects although rigid polymethacrylate backbones have a higher energy barrier for the exchange of polymer chains. In fact, the acrylate-random copolymer micelles induced chain exchange even at 10 °C (Fig. 7), whereas their methacrylate-random copolymer counterparts required a temperature at least above 25 °C for efficient chain exchange.⁵³ We thus revealed that the flexible acrylate random copolymers were effective for the design of size- and aggregation number-controlled micelles with low CMC yet dynamic chain exchange properties even at low temperature.

Conclusions

In summary, we investigated the self-assembly of acrylate-based amphiphilic random copolymers into micelles in water, focusing on the micelle size and aggregation number, CMC, and dynamic exchange behaviour of polymer chains. Multichain micelles with almost constant size (M_w and R_h) were formed below a threshold DP_{th} and unimer micelles were mainly formed above the DP_{th} . The constant M_w and DP_{th} for the multichain micelles increased with the content of hydrophobic dodecyl groups. The CMC of the random copolymers in water was approximately 1×10^{-3} mg mL⁻¹ regardless of the DP and monomer sequence, indicative of the stable formation of micelles at low concentration. Uniquely, the flexible acrylate random copolymer micelles induced the exchange of polymer chains in water even at a low temperature such as 10 °C, though relatively rigid methacrylate random copolymers required at least 25 °C for efficient chain exchange. The chain exchange was promoted by increasing temperature and N_{agg} . Thus, the self-assembly of flexible acrylate-based random copolymers in water is suitable for the design of size-controlled micelles with dynamic chain exchange properties even at low temperature; such dynamic yet precise self-assemblies would be useful as encapsulation/release materials or delivery vessels for various applications.

Data availability

The data supporting this study have been included as part of the ESI.† Experimental details of the synthesis and characteriz-

ation of polymers and SEC, NMR, DLS, and fluorescence spectroscopy.

Conflicts of interest

There are no conflicts to declare.

Acknowledgements

This work was supported by Japan Society for the Promotion of Science KAKENHI grants (JP19K22218, JP20H02787, JP20H05219, JP22H04539, JP23H02008, and JP23K26701), JST PRESTO grant number JPMJPR24M6, Ogasawara Foundation for the Promotion of Science & Engineering, the Noguchi Institute, the Institute for Chemical Fibers, Japan, Iketani Science and Technology Foundation, Kurita Water and Environment Foundation.

References

- 1 L. Zhang and A. Eisenberg, *Science*, 1995, **268**, 1728–1731.
- 2 B. M. Discher, Y. Y. Won, D. S. Ege, J. C. M. Lee, F. S. Bates, D. E. Discher and D. A. Hammer, *Science*, 1999, **284**, 1143–1146.
- 3 D. E. Discher and A. Eisenberg, *Science*, 2002, **297**, 967–973.
- 4 Z. Li, E. Kesselman, Y. Talmon, M. A. Hillmyer and T. P. Lodge, *Science*, 2004, **306**, 98–101.
- 5 R. K. O'reilly, C. J. Hawker and K. L. Wooley, *Chem. Soc. Rev.*, 2006, **35**, 1068–1083.
- 6 A. O. Moughton, M. A. Hillmyer and T. P. Lodge, *Macromolecules*, 2012, **45**, 2–19.
- 7 Y. Mai and A. Eisenberg, *Chem. Soc. Rev.*, 2012, **41**, 5969–5985.
- 8 Y. Lu, J. Lin, L. Wang, L. Zhang and C. Cai, *Chem. Rev.*, 2020, **120**, 4111–4140.
- 9 T. Terashima, *Polym. J.*, 2014, **46**, 664–673.
- 10 S. Mavila, I. Rozenberg and N. G. Lemcoff, *Chem. Sci.*, 2014, **5**, 4196–4203.
- 11 M. Gonzalez-Burgos, A. Latorre-Sanchez and J. A. Pomposo, *Chem. Soc. Rev.*, 2015, **44**, 6122–6142.
- 12 P. W. Roesky and C. Barner-kowollik, *Polym. Chem.*, 2015, **6**, 4358–4365.
- 13 C. Song, L. Li, L. Dai and S. Thayumanavan, *Polym. Chem.*, 2015, **6**, 4828–4834.
- 14 A. M. Hanlon, C. K. Lyon and E. B. Berda, *Macromolecules*, 2016, **49**, 2–14.
- 15 S. Mavila, O. Eivgi, I. Berkovich and N. G. Lemcoff, *Chem. Rev.*, 2016, **116**, 878–961.
- 16 O. Altintas and C. Barner-Kowollik, *Macromol. Rapid Commun.*, 2016, **37**, 29–46.
- 17 E. S. Gil and S. M. Hudson, *Prog. Polym. Sci.*, 2004, **29**, 1173–1222.
- 18 F. D. Jochum and P. Theato, *Chem. Soc. Rev.*, 2013, **42**, 7468–7483.

- 19 M. I. Gibson and R. K. O'reilly, *Chem. Soc. Rev.*, 2013, **42**, 7204–7213.
- 20 A. P. Esser-Kahn, S. A. Odom, N. R. Sottos, S. R. White and J. S. Moore, *Macromolecules*, 2011, **44**, 5539–5553.
- 21 Z. Jiang, H. Liu, H. He, A. E. Ribbe and S. Thayumanavan, *Macromolecules*, 2020, **53**, 2713–2723.
- 22 K. Kataoka, A. Harada and Y. Nagasaki, *Adv. Drug Delivery Rev.*, 2012, **64**, 37–48.
- 23 N. Kamaly, B. Yameen, J. Wu and O. C. Farokhzad, *Chem. Rev.*, 2016, **116**, 2602–2663.
- 24 Y. Wang, C. M. Kausch, M. Chun, R. P. Quirk and W. L. Mattice, *Macromolecules*, 1995, **28**, 904–911.
- 25 P. Bhargava, J. X. Zheng, P. Li, R. P. Quirk, F. W. Harris and S. Z. D. Cheng, *Macromolecules*, 2006, **39**, 4880–4888.
- 26 R. Lund, L. Willner, J. Stellbrink, P. Lindner and D. Richter, *Phys. Rev. Lett.*, 2006, **96**, 1–4.
- 27 T. P. Lodge, C. L. Seitzinger, S. C. Seeger, S. Yang, S. Gupta and K. D. Dorfman, *ACS Polym. Au*, 2022, **2**, 397–416.
- 28 H. Yamamoto and Y. Morishima, *Macromolecules*, 1999, **32**, 7469–7475.
- 29 H. Yamamoto, I. Tomatsu, A. Hashidzume and Y. Morishima, *Macromolecules*, 2000, **33**, 7852–7861.
- 30 S. Yusa, A. Sakakibara, T. Yamamoto and Y. Morishima, *Macromolecules*, 2002, **35**, 10182–10188.
- 31 T. Kawata, A. Hashidzume and T. Sato, *Macromolecules*, 2007, **40**, 1174–1180.
- 32 K. Dan, N. Bose and S. Ghosh, *Chem. Commun.*, 2011, **47**, 12491–12493.
- 33 L. Li, K. Raghupathi, C. Song, P. Prasad and S. Thayumanavan, *Chem. Commun.*, 2014, **50**, 13417–13432.
- 34 R. Nakahata and S. I. Yusa, *Langmuir*, 2019, **35**, 1690–1698.
- 35 Y. Hirai, T. Terashima, M. Takenaka and M. Sawamoto, *Macromolecules*, 2016, **49**, 5084–5091.
- 36 G. Hattori, Y. Hirai, M. Sawamoto and T. Terashima, *Polym. Chem.*, 2017, **8**, 7248–7259.
- 37 G. Hattori, M. Takenaka, M. Sawamoto and T. Terashima, *J. Am. Chem. Soc.*, 2018, **140**, 8376–8379.
- 38 Y. Kimura, T. Terashima and M. Sawamoto, *Macromol. Chem. Phys.*, 2017, **218**, 1700230.
- 39 S. Imai, Y. Hirai, C. Nagao, M. Sawamoto and T. Terashima, *Macromolecules*, 2018, **51**, 398–409.
- 40 M. Shibata, M. Matsumoto, Y. Hirai, M. Takenaka, M. Sawamoto and T. Terashima, *Macromolecules*, 2018, **51**, 3738–3745.
- 41 S. Imai, M. Takenaka, M. Sawamoto and T. Terashima, *J. Am. Chem. Soc.*, 2019, **141**, 511–519.
- 42 M. Hibino, K. Tanaka, M. Ouchi and T. Terashima, *Macromolecules*, 2022, **55**, 178–189.
- 43 M. Hibino, S. I. Takata, K. Hiroi, H. Aoki and T. Terashima, *Macromolecules*, 2023, **56**, 2955–2964.
- 44 D. Taura, A. Hashidzume, Y. Okumura and A. Harada, *Macromolecules*, 2008, **41**, 3640–3645.
- 45 D. Taura, Y. Taniguchi, A. Hashidzume and A. Harada, *Macromol. Rapid Commun.*, 2009, **30**, 1741–1744.
- 46 M. Ueda, A. Hashidzume and T. Sato, *Macromolecules*, 2011, **44**, 2970–2977.
- 47 K. Uramoto, R. Takahashi, K. Terao and T. Sato, *Polym. J.*, 2016, **48**, 863–867.
- 48 H. Kono, M. Hibino, D. Ida, M. Ouchi and T. Terashima, *Macromolecules*, 2023, **56**, 6086–6098.
- 49 K. Kalyanasundaram and J. K. Thomas, *J. Am. Chem. Soc.*, 1977, **99**, 2039–2044.
- 50 M. Wilhelm, C. Le Zhao, Y. Wang, R. Xu, M. A. Winnik, J. L. Mura, G. Riess and M. D. Croucher, *Macromolecules*, 1991, **24**, 1033–1040.
- 51 P. Raffa, D. A. Z. Wever, F. Picchioni and A. A. Broekhuis, *Chem. Rev.*, 2015, **115**, 8504–8563.
- 52 A. Goswami, G. Verma, P. A. Hassan and S. S. Bhagwat, *J. Dispersion Sci. Technol.*, 2015, **36**, 885–891.
- 53 R. Kanno, H. Kono, A. Ryoki, M. Ouchi and T. Terashima, *J. Am. Chem. Soc.*, 2024, **146**, 30848–30859.